Spring 2010

Magnetostratigraphy of the Hell Creek and lower Fort Union formations in northeast Montana

Rebecca LeCain
University of New Hampshire, Durham

MAGNETOSTRATIGRAPHY OF THE HELL CREEK AND LOWER FORT UNION FORMATIONS IN NORTHEAST MONTANA

BY

REBECCA LECAIN

THESIS

Submitted to the University of New Hampshire

In Partial Fulfillment of

The Requirements for the Degree of

Master of Science

In

Earth Sciences

May, 2010

ProQuest LLC
789 East Eisenhower Parkway
P.O. Box 1346
Ann Arbor, MI 48106-1346

This thesis has been examined and approved.

Thesis Director William Clyde, Associate Professor of Geology

Joel Johnson, Assistant Professor of Geology

Gregory P. Wilson, Assistant Professor of Biology, University of Washington

5/4/10

Date

TABLE OF CONTENTS

ACKNOWLEDGMENTS

In addition to my committee members, I would like to thank Jeremy Riedel for collecting and organizing the GPS measurements and Matt Jones for assisting with field work. Funding for this research was provided by NSF grant EAR0642291 and assistantships from the UNH Earth Sciences Department.

LIST OF TABLES

TABLE PAGE

LIST OF FIGURES

FIGURE PAGE

ABSTRACT

MAGNETOSTRATIGRAPHY OF THE HELL CREEK AND LOWER FORT UNION FORMATIONS IN NORTHEAST MONTANA

by

Rebecca LeCain

University of New Hampshire, May 2010

Magnetostratigraphic evaluation of a well-exposed stratigraphic section in northeast Montana has been undertaken to expand upon and better understand the timing of the deposition of Hell Creek and Fort Union Formations. Characteristic remnant magnetizations show clear magnetostratigraphic patterning of chrons C28n, C28r, C29n, C29r, C30n, and possibly C30r. Differentially corrected GPS coordinates, including elevation, were recorded at each sample site allowing the magnetostratigraphic framework to be precisely relocated in the field and traced laterally across the landscape. Localities in Montana that have been sampled for fossil studies have been mapped and correlated to the same stratigraphic sections as the magnetostratigraphy, and so can be compared directly to the geomagnetic polarity time scale. The new magnetostratigraphy can also be used to relate to other basins of Cretaceous and Paleogene age using information independent from biostratigraphic zonation, making it possible to directly compare the composition of coeval faunas from significantly different latitudes.

INTRODUCTION

The Hell Creek and Fort Union Formations extend across portions of Montana, Wyoming, North Dakota and South Dakota, within the Williston Basin which is a large Laramide foreland basin (Figure 1). These units preserve a particularly complete record of a late Cretaceous to early Paleocene continental ecosystem. The Hell Creek Formation is composed of "...poorly-cemented fine-grained sandstone, siltstone, carbonaceous-rich shale, mudstone, claystone, and the occasional lignite... These were laid down in a broad, fluvial, highly-vegetated plain that was dissected by meandering rivers that often overflowed their banks." (Murphy et al, 2002, p.9 and p.30). Below the Hell Creek Formation is the primarily marine Fox Hills Formation. The contact between the two formations may represent a regional unconformity, although this has not been verified (Murphy et al, 2002). In many places, tuff deposits from the base of the Hell Creek Formation have proved difficult to date because of detrital potassium feldspars which misrepresent the age of the limited volcanic material (Hicks et al, 2002). Because of this, determining exactly when Hell Creek deposition began is problematic.

The lithologies of the overlying Fort Union Formation include sandstones, shales and extensive coal beds, that were also laid down in fluvial and lacustrine settings, albeit relatively poorly drained ones than during the Hell Creek Formation. The fluvial channels of both formations tended to collect and concentrate organisms and bones so both formations are important sources for

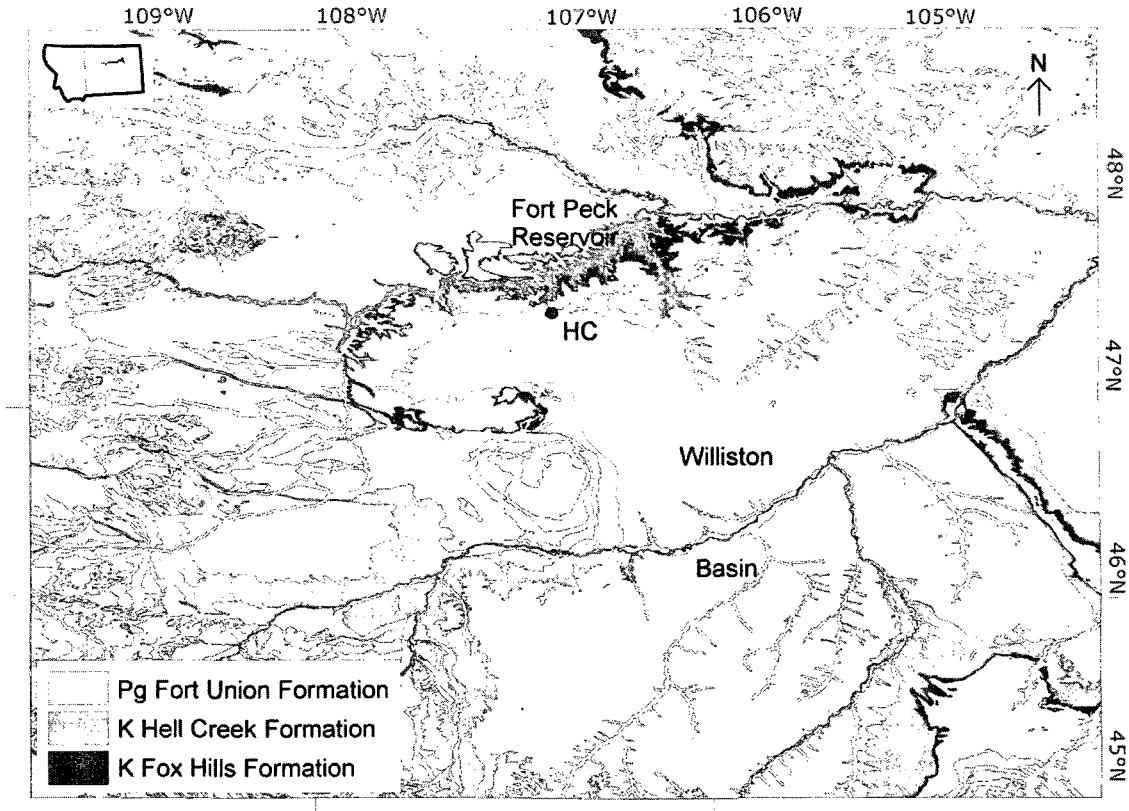

Figure 1. Simplified geologic map of eastern Montana. The red dot at HC is the location of the proposed type section for the Hell Creek Formation at Flag Butte.

fossils. Some of the best preserved late Cretaceous dinosaurs and early Paleogene mammals are preserved in these units (Clemens, 2002; Hartman, 2002; Wilson, 2005). However, these channel deposits do not extend laterally very far and so it is difficult to correlate rock types in different areas. The rivers flowed into the intercontinental sea that covered much of North America during the Cretaceous, and finally retreated from the area at the end of the Cretaceous (Murphy et al., 2002). The Cretaceous-Paleogene (K-Pg) boundary in this region follows the Hell Creek-Fort Union contact, is well preserved and includes indicators of impact and extinction (Hartman, 2002). Because of this, the boundary has been extensively studied with different dating techniques to constrain its timing; however, time constraints farther away from the boundary are more limited in both formations (Hicks et al., 2002; Swisher et al., 1993). Where the rocks have been dated, they frequently have not been correlated to fossil finds directly, so it is difficult to determine a precise age for many of the fossils from this region.

This study evaluates the magnetostratigraphy of several late Cretaceous to early Paleogene stratigraphic sections in the Fort Peck area of northeast Montana. The study area includes the proposed type section for the Hell Creek Formation at Flag Butte as well as several important fossil vertebrate localities in the Fort Union Formation. Paleomagnetic sample sites also have precise differentially corrected GPS locations so they can be easily relocated and tied to future paleontological studies. By providing a chronostratigraphic framework for the many fossil collections in the region it will allow more precise study of

terrestrial ecosystem change across the K/Pg boundary and enable correlation of early Paleogene mammals in the Western Williston Basin to those in other basins, potentially providing a better temporal framework for the radiation of early mammals.

CHAPTER I

METHODS

Paleomagnetic sampling was undertaken in four sections chosen to maximize relevance to local paleontological studies and minimize redundancy to previous paleomagnetic studies (Greg Wilson, personal correspondence; Wilson, 2005). The stratigraphically lowest section, East Ried Coulee (ERC) to Flag Butte is also within the proposed type locality for the Hell Creek Formation (Hartman, in preparation). In order to measure stratigraphic sections, differential GPS was used to measure the elevation of major lithological boundaries, and the intervening thicknesses were also measured by Jacob-staff for comparison. Discrepancies in thickness between the two methods are on the centimeter scale; therefore GPS elevations are comparable to Jacob-staffing in providing lithological thickness and have the added benefit of giving absolute elevation.

At each of the 47 paleomagnetic sampling sites, four or more oriented hand samples were collected by removing overlying cover so that the samples could be taken from the underlying rock layers that had not experienced surface weathering. Differential GPS coordinates (latitude, longitude, elevation) were also recorded for each sample site. The three most intact hand samples from each location were sanded into $8cm^3$ cubes, demagnetized using a Molspin tumbling alternating field (AF) demagnetizer, and analyzed with the HSM2 SQUID-based spinner magnetometer at the University of New Hampshire.

Demagnetization protocol and interpretation of magnetic mineralogy were based on previously published magnetostratigraphic studies from these units (Lund et al., 2002; Swisher et al., 1993) and on an initial round of pilot results where each sample was demagnetized by 2.5mT steps, up to 100mT

CHAPTER II

PALEOMAGNETIC RESULTS

AF demagnetization produced stable results for the majority of samples. Samples with clear overprint and characteristic remanent magnetizations (ChRM) comprised 69% of the total samples and were evaluated using principal components analysis (Kirschvink, 1980; Fig. 2A, 2B). In 11% of the samples, the higher coercivity vector end points cluster together rather than trend towards the origin (Fig. 2C, 2D). For these samples, the characteristic component was analyzed using a Fisher mean (Fisher, 1953). The demagnetization data for the other 20% of the samples lay within a plane where linear demagnetization was obscured by overlapping unblocking spectra (Fig. 2E, 2F). Directions for these were found by calculating the point on the great circle path from the overprint direction to the characteristic direction that lies closest to the overall mean direction from the better determined sites.

At site MT0807, samples were taken from mud clasts within a sandstone for the purpose of applying the conglomerate test (Figure 3). The calculated declinations and inclinations from each sample at this site were significantly different from one another and from the modern magnetic field indicating that the remanent magnetization is likely from original deposition of the muds and not from later overprinting fields (Table 1). A large within-site spread of characteristic directions occurred in sites MT0809, MT0820, MT0823, and MT0825; so

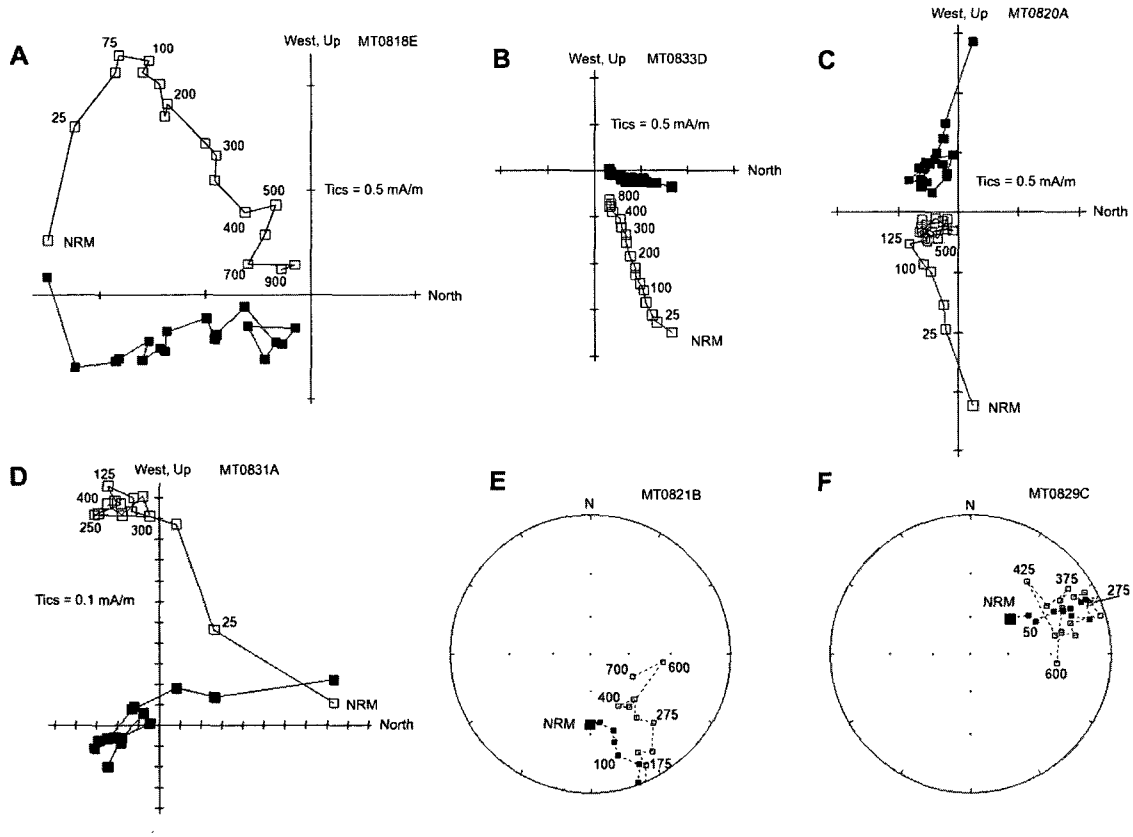

Figure 2. Demagnetization of representative samples from the Hell Creek (A, C, E) and Fort Union (B, D, F) Formations. A and B trend in a line towards the origin, C and D cluster and were evaluated using a Fisher Mean, and E and F were analyzed using the calculated great circle. Open symbols represent vector end points in the vertical plane and closed symbols are in the horizontal plane (Zijderveld, 1967). Open symbols in the equal area projections (E, F) are on the upper hemisphere; closed symbols on the lower hemisphere.

summary statistics were not calculated for those sites. Site localities with samples that exhibited stable demagnetization behavior were categorized as either alpha or beta sites and summary statistics were calculated from these sites (Table 2). Sites that passed Watson's (1956) test of randomness at the 95% confidence level and where either all three samples were interpreted using principle components analysis or one of the three sample was characterized by a mean direction, were considered alpha sites (Fig. 4). Beta sites contained samples characterized by more than one mean direction or any great circle paths. A reversal test of the alpha sites shows that they are close to antipodal, but do not pass at the 95% confidence interval, likely due to incomplete removal of modern normal overprint that leads to overly shallow reverse polarity directions. The mean VGP of the alpha sites is lat/long 76.5/136.8, α_{95} = 7.5, which is close to but not overlapping with the late Cretaceous North American pole from Besse and Courtillot's (2002) study of 73.5/207.3, α_{95}=3.6. This discrepancy of expected and actual paleomagnetic poles can also be explained by the overly shallow reverse polarity directions noted above. There is no significant tilt of the Hell Creek or Fort Union Formations in this area, so no tilt corrections were calculated for the summary statistics.

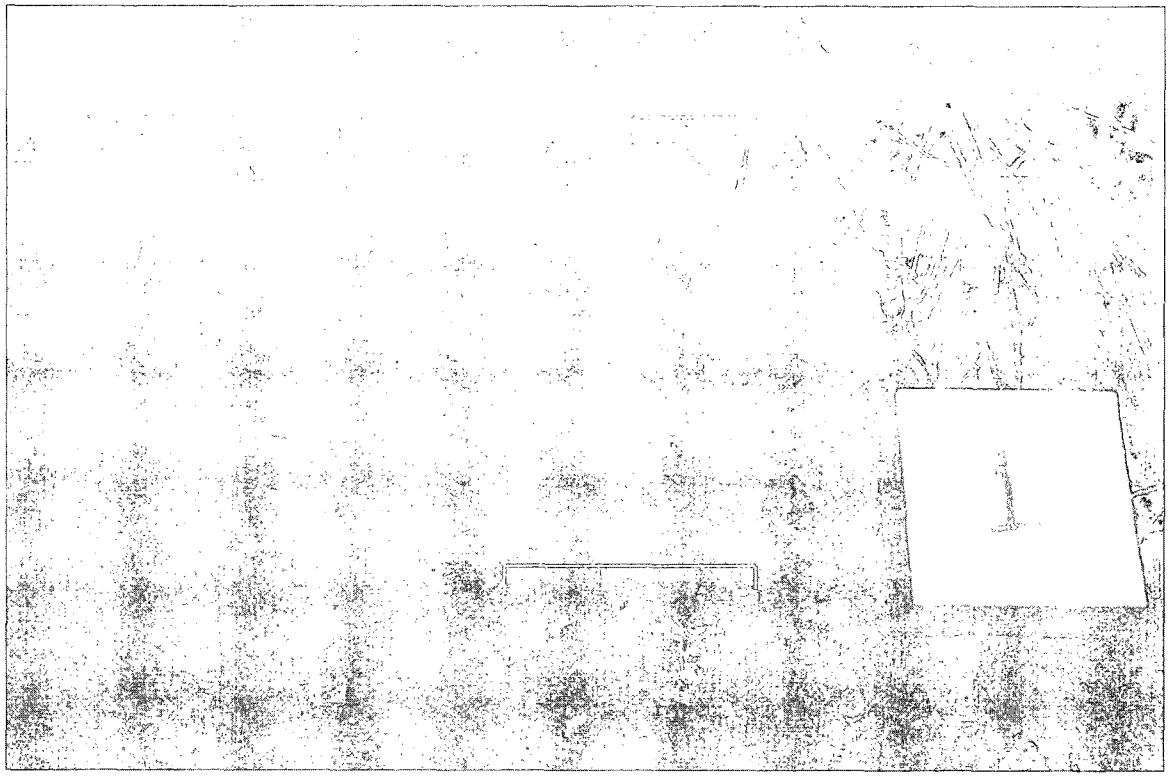

Figure 3. Photograph of mudstone clasts (under brackets) within sandstone at site MT0807. Edge of notepad is 3.5cm for scale.

TABLE 1. PALEOMAGNETIC RESULTS OF SAMPLES FROM SITE MT0807

Sample	Declination	Inclination	Longitude (dec. deg.)	Latitude (dec. deg.)	VGP long.	VGP lat.
MT0807A	70.9	-22	-106.881	47.55852	4.9	4.0
MT0807C	177.4	67	-106.881	47.55852	254.8	7.3
MT0807D	214.6	-84	-106.881	47.55852	85.4	-56.8

TABLE 2.

Site Number	Section	Site Type	Longitude (dec.deg.)	Latitude (dec.deg.)	Elevation (m)	Height in section (m)	Geo Dec	Geo Inc	R	k	α95	VGP long.	VGP lat.	Chron
mt0801	ERC-F	alpha	-106.88172	47.56443	714.08	0.00	160.8	-42.6	2.96	56.45	16.6	293.5	-62.5	30r
mt0802	ERC-F	alpha	-106.88172	47.56443	715.18	1.10	187.0	-70.0	2.96	46.00	18.4	105.2	-82.2	30r
mt0803	ERC-F	alpha	-106.88150	47.56484	721.70	7.63	144.5	-22.4	2.91	22.65	26.5	304.6	-43.4	30r
mt0804	ERC-F	alpha	-106.88160	47.56481	724.88	10.81	15.0	35.2	2.99	141.57	10.4	44.5	59.3	30n
mt0805	ERC-F	alpha	-106.88160	47.56487	727.05	12.98	19.4	26.2	2.96	50.10	17.6	41.0	52.6	30n
mt0806	ERC-F	beta	-106.88124	47.56410	726.55	12.48	27.5	64.1	2.33	2.97	90.3	338.1	71.2	30n
mt0807	ERC-F	NA	-106.88120	47.56409	732.59	18.52	NA	NA	NA	NA	NA	NA	NA	30n
mt0808	ERC-F	alpha	-106.87992	47.56333	748.32	34.25	3.1	63.6	2.98	132.97	10.7	29.7	86.8	30n
mt0809	ERC-F	NA	-106.87247	47.56032	752.27	38.20	NA	NA	NA	NA	NA	NA	NA	30n
mt0810	ERC-F	alpha	-106.87278	47.56032	757.57	43.49	326.8	65.4	2.96	50.22	17.6	175.4	67.8	30n
mt0811	ERC-F	alpha	-106.87306	47.56029	760.56	46.49	349.2	56.2	2.92	23.89	25.8	113.4	76.6	30n
mt0812	ERC-F	alpha	-106.87174	47.55903	764.05	49.97	318.3	61.4	2.99	192.51	8.9	168.9	60.5	30n
mt0813	ERC-F	alpha	-106.86984	47.55848	776.49	62.41	359.9	73.4	2.99	142.45	10.4	252.9	78.4	30n
mt0814	ERC-F	alpha	-106.86994	47.55813	781.31	67.23	5.7	71.8	2.90	20.16	28.2	271.9	80.2	30n
mt0815	ERC-F	alpha	-106.87097	47.55831	788.46	74.38	358.4	53.5	2.92	25.5	24.9	78.8	76.4	30n
mt0816	ERC-F	alpha	-106.87088	47.55820	792.86	78.78	350.0	57.2	2.95	37.24	20.5	113.6	77.8	30n
mt0817	ERC-F	beta	-106.87083	47.55817	794.59	80.51	351.2	65.4	2.13	2.31	114.3	166.0	84.1	30n
mt0818	ERC-F	alpha	-106.86960	47.55670	814.84	100.77	149.9	-33.6	2.73	7.46	48.8	303.6	-51.9	29r
mt0819	ERC-F	beta	-106.86953	47.55666	816.69	102.61	199.3	-62.5	2.72	7.22	49.7	171.4	-76.1	29r
mt0820	ERC-F	NA	-106.86950	47.55665	817.69	103.61	NA	NA	NA	NA	NA	NA	NA	29r
mt0821	ERC-F	beta	-106.86944	47.55663	819.13	105.06	145.9	-55.4	2.95	44.15	18.8	330.8	-62.3	29r
mt0822	ERC-F	alpha	-106.86998	47.55634	820.13	106.06	126.7	-31.2	2.99	158.72	9.8	326.7	-36.9	29r
mt0823	ERC-F	NA	-106.86957	47.55611	827.47	113.39	NA	NA	NA	NA	NA	NA	NA	29r
mt0824	ERC-F	alpha	-106.86957	47.55611	830.97	116.89	146.2	-38.9	2.97	59.94	16.1	311.6	-52.8	29r
mt0825	ERC-F	NA	-106.86948	47.55619	831.04	116.96	NA	NA	NA	NA	NA	NA	NA	29r

TABLE 2. *CONTINUED*

Site Number	Section	Site Type	Longitude (dec.deg.)	Latitude (dec.deg.)	Elevation (m)	Height in section (m)	Geo Dec	Geo Inc	R	k	α95	VGP long.	VGP lat.	Chron
mt0826	PL	beta	-107.05745	47.52408	859.42	0.00	154.8	-73.2	2.87	15.72	32.2	29.6	-71.3	29r
mt0827	PL	alpha	-107.05733	47.52394	863.56	4.14	147.0	-34.2	2.91	23.14	26.2	307.4	-50.7	29r
mt0828	PL	alpha	-107.05741	47.52372	865.22	5.80	168.2	-30.4	2.97	71.36	14.7	274.3	-57.4	29r
mt0829	PL	beta	-107.05734	47.52373	868.51	9.08	201.1	-73.8	2.94	34.31	21.4	110.1	-72.6	29r
mt0830	PL	beta	-107.05712	47.52369	874.40	14.98	166.0	-61.3	2.95	40.52	19.6	320.7	-78.9	29r
mt0831	PL	beta	-107.05681	47.52361	877.20	17.77	195.2	-64.0	2.99	286.88	7.3	167.1	-79.4	29r
mt0832	PL	alpha	-107.05682	47.52345	881.39	21.94	353.0	68.9	2.88	16.79	31.1	212.6	83.4	29n
mt0833	PL	alpha	-107.05691	47.52341	883.43	24.00	14.9	68.3	3.00	448.98	5.8	315.1	79.6	29n
mt0834	GH	alpha	-107.06822	47.51590	883.96	2.00	278.3	65.3	2.95	41.05	19.5	195.3	37.5	29n
mt0835	GH	alpha	-107.06806	47.51552	888.82	6.86	356.3	59.9	2.99	233.78	8.1	95.8	82.8	29n
mt0836	GH	alpha	-107.06796	47.51545	892.97	11.01	354.0	60.9	2.99	188.13	9.0	112.5	83.0	29n
mt0837	PL	alpha	-107.05712	47.52357	879.68	20.25	169.0	-52.8	2.93	28.31	23.6	287.3	-73.6	29r
mt0838	MD(GH)	alpha	-107.05942	47.51980	883.44	1.48	314.7	70.2	2.97	66.14	15.3	193.5	61.2	29n
mt0839	GH	alpha	-107.06786	47.51540	897.49	15.53	320.6	61.9	2.97	74.20	14.4	168.6	62.3	29n
mt0840	GH	alpha	-107.06780	47.51540	899.42	17.46	338.9	75.7	2.98	119.76	11.3	223.5	70.6	29n
mt0841	W-BB	alpha	-107.08008	47.50855	904.15	0.00	35.5	58.8	2.98	89.47	13.1	347.1	63.3	29n
mt0842	W-BB	alpha	-107.07996	47.50893	916.54	12.39	327.8	62.9	2.97	78.28	14.0	166.8	67.5	29n
mt0843	W-BB	beta	-107.06884	47.48754	918.71	14.56	153.8	-52.7	2.57	4.67	65.0	316.6	-65.7	28r
mt0844	W-BB	alpha	-107.06865	47.48748	924.01	19.86	167.5	-61.2	2.96	48.42	17.9	316.9	-79.7	28r
mt0845	W-BB	beta	-107.06778	47.48658	936.83	32.68	334.8	59.0	2.64	5.49	58.6	149.1	70.3	28n
mt0846	W-BB	alpha	-107.06777	47.48654	939.55	35.40	337.9	57.7	2.96	44.49	18.7	141.3	71.5	28n
mt0847	W-BB	alpha	-107.08005	47.50891	917.62	13.47	351.1	64.9	2.99	140.94	10.4	160.1	83.9	29n

Table 2. Summary site statistics. ERC-F = East Ried Coulee to Flag Butte Section; PL = Pearl Lake Section; GH = Garbani Hill Section, where MD = McDonald Quarry; W-BB = W Coal Area to Biscuit Butte Section.

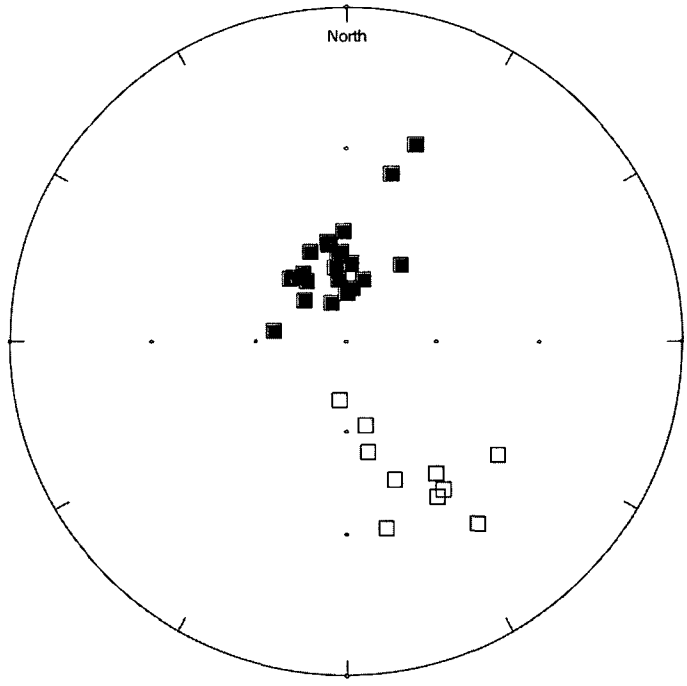

Figure 4. Equal-area projection of alpha site mean characteristic directions. Mean VGP (latitude/longitude) of 76.5/136.8 is close to the expected VGP of 73.5/207.3 (Besse and Courtillot, 2002). Filled squares represent normal polarity sites, open are reverse polarity sites.

CHAPTER III

MAGNETOSTRATIGRAPHIC RESULTS

East Ried Coulee to Flag Butte Section

The 117m section extending from East Ried Coulee (ERC) in the northwest to Flag Butte in the southeast (Figure 5) contains the upper Fox Hills Formation and the entirety of the Hell Creek Formation. The Hell Creek Formation in this area is 92.1m thick (Appendix A). The 25 paleomagnetic sites collected and analyzed from this section indicate two magnetic reversals, from reverse polarity to normal and back to reverse polarity (Figure 6). The lignite bed that is characteristic of the K-Pg boundary in this area is located at the very top of this section, within the upper reversed zone interpreted to be C29r (Ogg and Smith, 2004). Between 16.19m and 36.45m below the K-Pg lignite is the first reversal, to a normal polarity zone, interpreted here to be C30n. The range where the reversal occurs is large due to a sandstone layer too coarse for accurate paleomagnetic analysis. Within the upper Fox Hills Formation is the second reverse polarity zone, possibly C30r (see discussion section below)

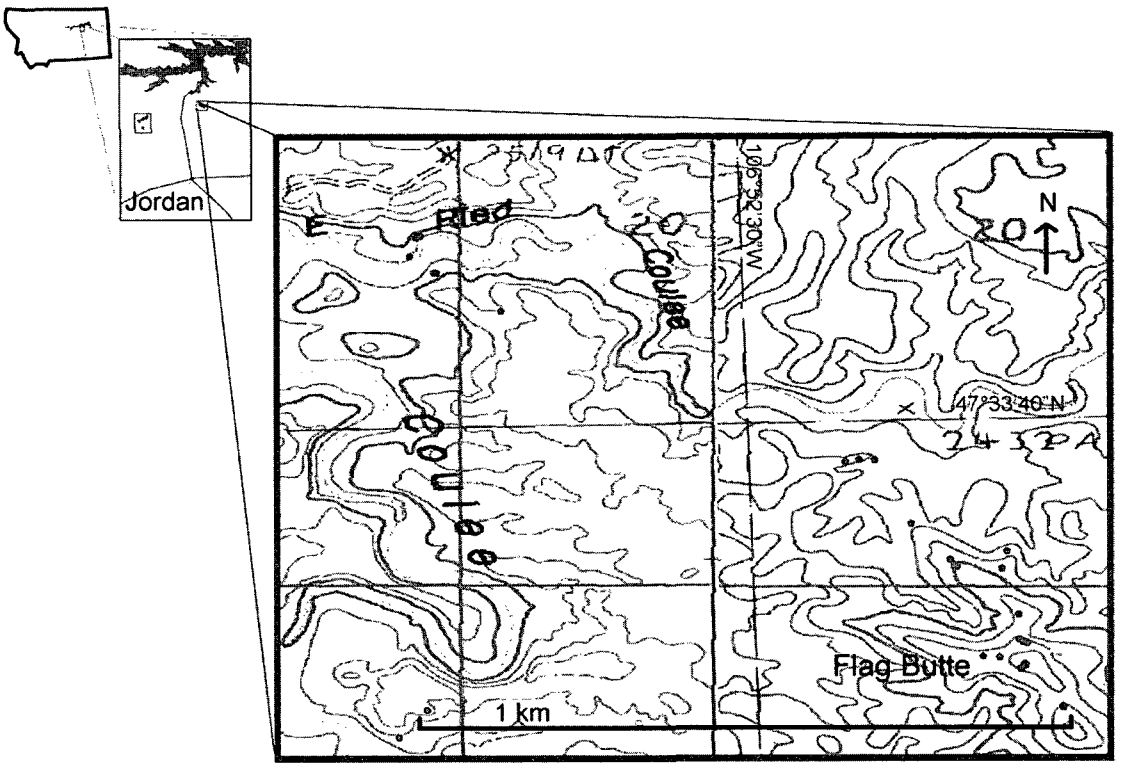

Figure 5. Map of eastern part of field area showing paleomagnetic sample sites (red dots) within the East Ried Coulee to Flag Butte Section.

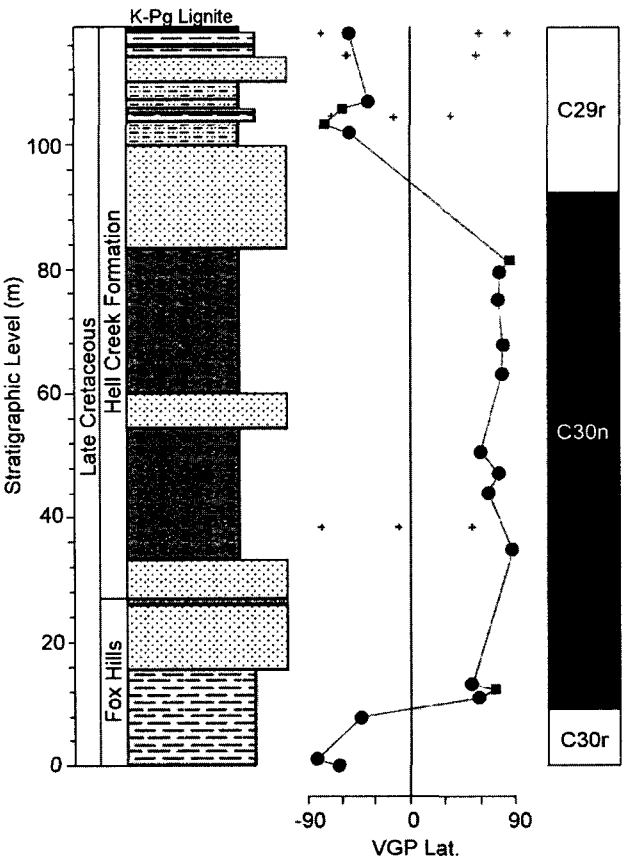

Figure 6. Stratigraphy, measured VGP latitudes and interpreted magnetostratigraphy of the East Ried Coulee to Flag Butte Section. Key same as Figure 8.

Pearl Lake Section

The northernmost section of the western part of the field area lies approximately 14.5km west of the ERC to Flag Butte Section (Figure 7). It is 24m thick (Appendix B), and contains nine paleomagnetic sample sites. The lower Z coal, which represents the K-Pg boundary in this area (Swisher et al., 1993), is 45cm thick and is 4m above the bottom of the section. The magnetostratigraphy of this section begins with a reversed polarity zone, representing chron C29r, and changes to normal polarity (C29n) at 21m in the section (Figure 8). The top lignite, a Y coal stringer, can be traced to the bottom of the Garbani Hill Section

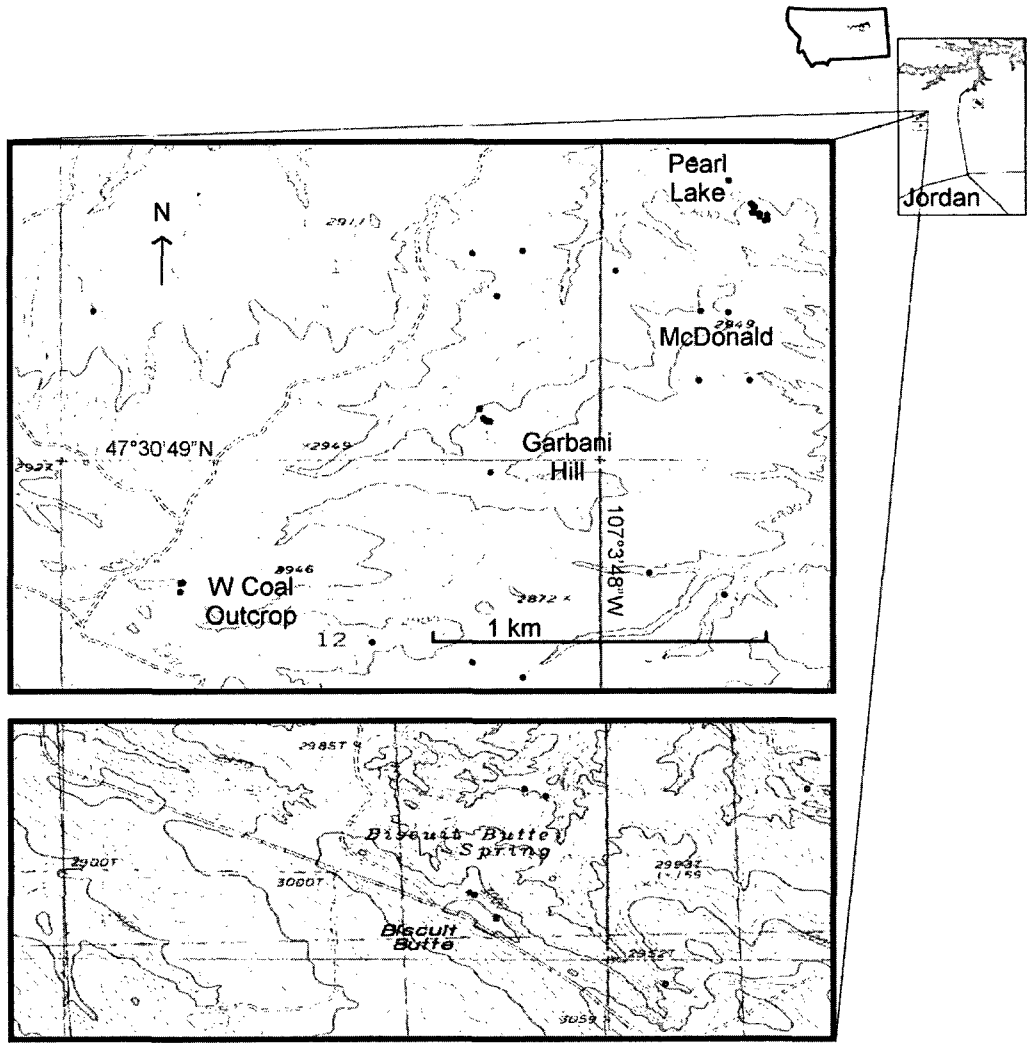

Figure 7. Map of western part of field area showing paleomagnetic sample sites (red dots and local fossil localities (green and purple dots) in Pearl Lake, Garbani Hill, and W Coal to Biscuit Butte Sections.

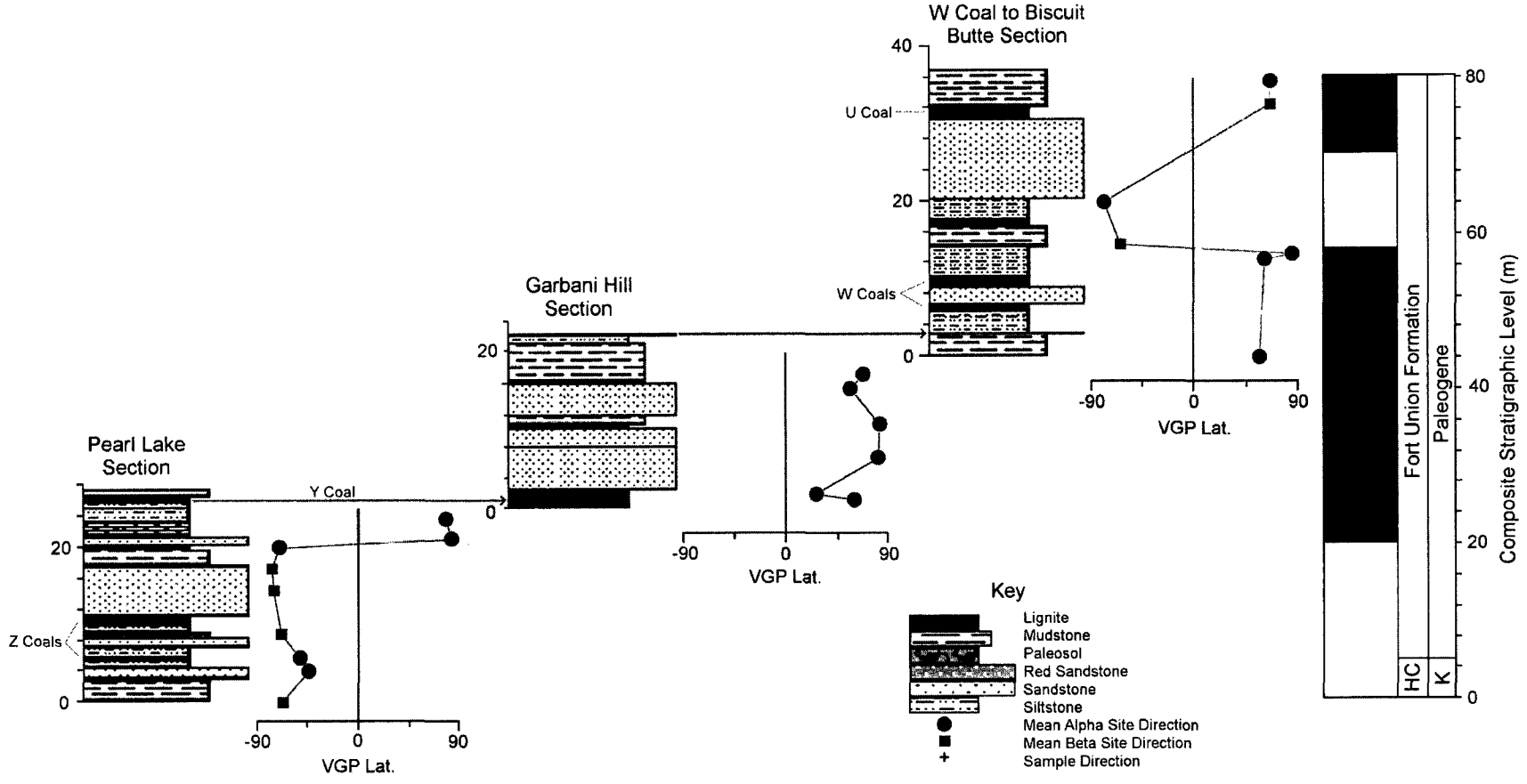

Figure 8. Stratigraphy, VGP latitudes and inferred magnetostratigraphy of Pearl Lake, Garbani Hill, and W coal to Biscuit Butte sections.

Garbani Hill Section

The Garbani Hill Section is 17.5m thick (Appendix C) and begins at the bottom of a hill next to the Garbani Channel Quarry (Clemens, 2002; Simmons, 1987). It extends from the 2m thick Y coal to a traceable thin red sandstone layer at the top of Garbani Hill. Five sites were sampled from Garbani Hill and one from McDonald quarry to the north (Figure 7). Paleomagnetic results show that this section is of entirely normal polarity and, given its lithostratigraphic overlap with the Pearl Lake Section, likely correlates to chron C29n (Figure 8).

W Coal area to Biscuit Butte Section

Seven sites were sampled from this 13.5m section (Appendix D) that begins near the W coal exposure next to the road on Engdahl's ranch going east from Snow Creek Road and extends to the top of Biscuit Butte (Figure 7). Paleomagnetic results indicate two reversals, from normal chron C29n to a thin reversed polarity zone (C28r), and back to a normal polarity zone interpreted to be chron C28n (Figure 8). This magnetostratigraphic pattern closely matches that found by Archibald et al. (1982) at their Biscuit Butte Section in this same area.

CHAPTER IV

DISCUSSION

Stratigraphy

In order to document the proposed type section for the Hell Creek Formation, Hartman (in preparation) completed a lithostratigraphic section near and on Flag Butte and found a total thickness for the Hell Creek Formation of 89.3m. This compares well with the 92.1m thickness found by this study. Several meter-scale sandstones serve as marker beds within the formation and can be correlated between the sections, despite some lateral differences in thickness (Hartman, personal correspondance). With the precise elevation measurements of differential GPS, the geometric properties of lithologic or chronostratigraphic boundaries can be determined over long distances. For instance, elevations from three points on the K-Pg boundary (Pearl Lake lower Z coal, Lerbekmo Hill lignite, and Flag Butte K-Pg lignite) define a chronostratigraphic plane on the landscape. From these measurements it was determined that the plane of the K-Pg boundary in this area dips less than 3° to the southeast (Figure 9). This dip is consistent with the study area's position on the northwestern edge of the Williston Basin. Using this stratigraphic model, it is

possible to estimate the elevation of the K-Pg boundary at any point in the region. This estimation, along with mean sedimentation rates between chron boundaries and elevation of fossil localities, can be used to estimate the ages of fossils in the region.

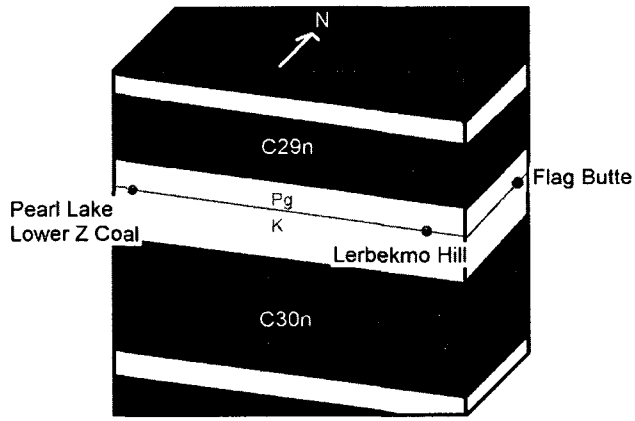

Figure 9. Block diagram of the chronostratigraphy of the study area inferred from the calculated dip of the K-Pg boundary. Diagram is schematic and vertically exaggerated.

Chron C30r

Previous Hell Creek magnetostratigraphic studies have largely concentrated on precisely dating the K-Pg boundary. Archibald et al. (1982) originally attempted to use magnetostratigraphy to correlate the Montana portion of the Williston Basin with the San Juan Basin in New Mexico and with Red Deer Valley in Alberta, but they did not extend the measurements taken from Montana to the lower boundary of the Hell Creek Formation. This information was then revised by Swisher et al. (1993) who extended magnetostratigraphic sampling to near the lower boundary of the Hell Creek Formation at Billy Creek (Figure 10). Two other studies that also extended sampling to the base of the Hell Creek Formation were located in eastern Montana (Lund et al. 2002) and in North Dakota (Hicks et al. 2002), where the Hell Creek Formation is thinner than in the west and may not contain as complete a stratigraphic record (Murphy et al., 2002). These studies found a large normal polarity interval in the lower half of the Hell Creek Formation which they interpreted either as one long polarity zone (C30n) or as two polarity zones (C30n + C31n) that could not be distinguished from one another due to sampling and stratigraphic incompleteness, thus they could not calculate a precise date for the beginning of sedimentation for the formation. More recently, Lerbekmo (2008) reported paleomagnetic results for the entirety of the Hell Creek and into the Fox Hills Formation and found a reverse polarity zone at the top of the Fox Hills Formation which he interpreted to be C30r. The same magnetostratigraphic pattern for the upper Fox Hills

Formation is found in this study, however a potential unconformity at the boundary of the Fox Hills and Hell Creek Formations (Murphy et al., 2002) makes it uncertain whether the normal polarity zone of the top of the Fox Hills Formation is part of the same chron as the normal polarity zone of the basal Hell Creek Formation. Without other age constraints on these portions of both formations, the identification of the normal polarity zones cannot be made with certainty. Although the assignment of the underlying reverse polarity zone to chron C30r is tenuous, it remains the most likely interpretation given the completeness of the rest of the section and the estimated duration of the sea-level cycle that led to the unconformity in the region (Lerbekmo, 2008).

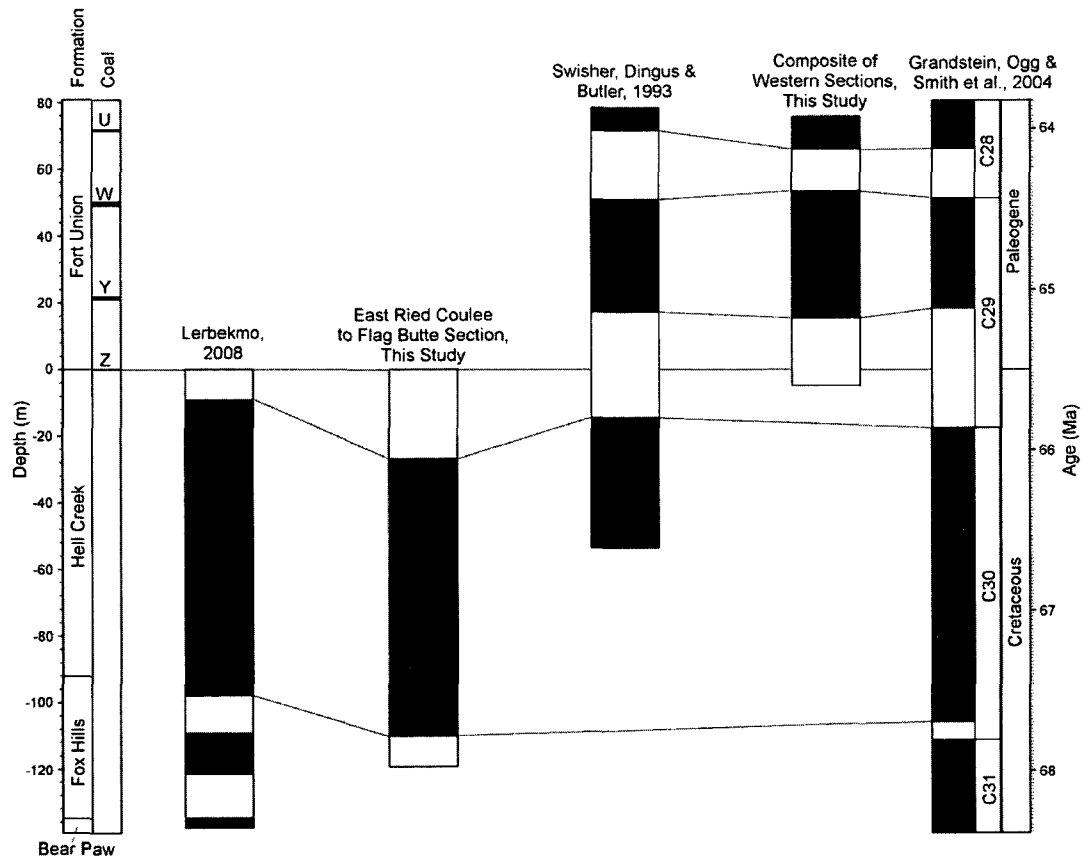

Figure 10. Fence diagram of previous magnetostratigraphic studies done in the study area compared to this study (Lerbekmo, 2008; Swisher et al., 1993).

Intrabasinal correlations

"A considerable level of biogeographic provinciality exists in the Puercan mammal age, especially between northern and southern faunas" (Lofgren et al., 2004), therefore it is important to use tools besides biostratigraphy to correlate between locations that have variable faunal compositions. In the Fort Peck Reservoir area of Montana, the Pu1 faunas of the Puercan North American land mammal age are found in the lower Fort Union Formation, and Pu2/3 indeterminate faunas have been found in the channel deposits of Garbani Quarry and Purgatory Hill. This is typical of northern Puercan localities, which largely consist of Pu1 faunas with some Pu3 and few Pu2 faunas (Lofgren, 2004). A thorough magnetostratigraphic and biostratigraphic analysis of the Puercan has been done on the Nacimiento Formation in the San Juan Basin, New Mexico (Williamson, 1996; Lofgren et al., 2004); however, the San Juan Basin has so far only yielded Pu2 and Pu3 faunas. The Hanna Basin in Wyoming does contain all three faunal groups, but these have yet to be linked to magnetostratigraphy (Lofgren, 2004). The magnetostratigraphy of this study extends from within chron 28 within which most of Pu3 can be found, to chron 29 which contains Pu1 and 2, which is similar to the findings in New Mexico (Lofgren et al., 2004; Williamson, 1996) so fossil studies can utilize this framework to determine the timing of faunal radiation of early mammals (Wilson, in preparation), and how the timing of diversification compares in northern versus southern regions of North America.

CHAPTER V

CONCLUSIONS

Four new magnetostratigraphic sections south of Fort Peck Reservoir in northeast Montana provide a record of chrons C28n through C30n and a reverse polarity zone tentatively interpreted as C30r. This magnetostratigraphy is directly linked to the proposed Hell Creek Formation type section on Flag Butte. The temporal model proposed here can be used to precisely interpolate ages of fossil localities in the lower Fort Union Formation and upper Hell Creek Formation. However, dating fossils within the lower Hell Creek Formation remains tentative until the ages of the upper Fox Hills Formation and the lower Hell Creek Fomation can be constrained, and the reverse polarity zone within the upper Fox Hills Formation can be concretely identified as C30r or C31r. These sections have the potential to add significant information to the dating of Puercan mammalian fossil localities, which is useful for correlation of fossil assemblages within early Paleocene basins and understanding the timing of early mammalian evolutionary radiation.

REFERENCES CITED

Archibald, J.D., Butler, R.F., Lindsay, E.H., Clemens, W.A., and Dingus, L., 1982. Upper Cretaceous-Paleocene biostratigraphy and magnetostratigraphy, Hell Creek and Tullock Formations, northeastern Montana. Geology v. 10, pp. 153-159.

Besse, J., and V. Courtillot, 2002. Apparent and true polar wander and the geometry of the geomagnetic field over the last 200 Myr, Journal of Geophysical Research, 107(B11).

Clemens, W.A., 2002. Evolution of the mammalian fauna across the Cretaceous-Tertiary boundary in northeastern Montana and other areas of the Western Interior, *in* Hartman, J.H., Johnson, K.R., and Nichols, D.J., eds., The Hell Creek Formation and the Cretaceous-Tertiary boundary, in the northern Great Plains: An integrated continental record of the end of the Cretaceous: Boulder, Colorado, Geological Society of America Special Paper 361, pp. 217-245.

Fisher, R. A., 1953. Dispersion on a sphere: Proceedings of the Royal Society, v. A217, pp. 295-305.

Hartman, J.H., 2002. Hell Creek Formation and the early picking of the Cretaceous-Tertiary boundary in the Williston Basin, *in* Hartman, J.H., Johnson, K.R., and Nichols, D.J., eds., The Hell Creek Formation and the Cretaceous-Tertiary boundary, in the northern Great Plains: An integrated continental record of the end of the Cretaceous: Boulder, Colorado, Geological Society of America Special Paper 361, pp.1-7.

Hicks, J.F., Johnson, K.R., Obradovich, J.D., Tauxe, L., and Clark, D., 2002. Magnetostratigraphy and geochronology of the Hell Creek and basal Fort Union Formations of southwestern North Dakota and a recalibration of the age of the Cretaceous-Tertiary boundary, *in* Hartman, J.H., Johnson, K.R., and Nichols, D.J., eds., The Hell Creek Formation and the Cretaceous-Tertiary boundary, in the northern Great Plains: An integrated continental record of the end of the Cretaceous, Boulder, Colorado, Geological Society of America Special Paper 361, pp. 35-55.

Kirschvink, J.L., 1980. The least-squares line and plane and the analysis of paleomagnetic data, Royal Astronomical Society Geophysical Journal, v. 62, pp. 743-746.

Lerbekmo, J.F., 2008. Glacioeustatic sea level fall marking the base of supercycle TA-1 at 66.5 Ma recorded by the kaolinization of the Whitemud Formation and the Colgate Member of the Fox Hills Formation, Marine and Petroleum Geology, pp. 1-5.

Lofgren, D.L., Lillegraven, J.A., Clemens, W.A., Gingerich, P.D., and Williamson, T.E., 2004. Paleocene Biochronology: The Puercan through Clarkforkian Land

Mammal Ages, *in* Late Cretaceous and Cenozoic Mammals of North America, ed. M.O. Woodburne. New York, NY: Columbia University Press, pp. 43-105.

Lund, S.P., Hartman, J.H., and Banerjee, S.K., 2002. Magnetostratigraphy of interfingering upper Cretaceous-Paleocene marine and continental strata of the Williston Basin, North Dakota and Montana, *in* Hartman, J.H., Johnson, K.R., and Nichols, D.J., eds., The Hell Creek Formation and the Cretaceous-Tertiary boundary, in the northern Great Plains: An integrated continental record of the end of the Cretaceous: Boulder, Colorado, Geological Society of America Special Paper 361, pp. 57-74.

Murphy, E.C., Hoganson, J.W., and Johnson, K.R., 2002. Lithostratigraphy of the Hell Creek Formation in North Dakota, *in* Hartman, J.H., Johnson, K.R., and Nichols, D.J., eds., The Hell Creek Formation and the Cretaceous-Tertiary boundary, in the northern Great Plains: An integrated continental record of the end of the Cretaceous: Boulder, Colorado, Geological Society of America Special Paper 361, pp. 9-34.

Ogg, J.G. and Smith, A.G., 2004. The geomagnetic polarity time scale, in A Geologic Time Scale 2004, eds. F.M. Gradstein, J.G. Ogg, and A.G. Smith. Cambridge University Press, pp. 63-86.

Simmons, N.B., 1987. A revision of Taeniolabis (Mammalia, Multituberculata) with a new species from the Puercan of eastern Montana. Journal of Paleontology 61, pp. 794-808.

Swisher, C.C., Dingus, L., Butler, R.F., 1993. Ar/Ar dating and magnetostratigraphic correlation of the terrestrial Cretaceous-Paleogene boundary and Puercan Mammal Age, Hell Creek-Tullock formations, eastern Montana. Canadian Journal of Earth Science 30, pp. 1981-1996.

Watson, G.S., 1956. A test for randomness of directions. Monthly Notices, Royal Astronomical Society, Geophysical Supplement, 7, 160-1.

Williamson, T.E., 1996. The Beginning of the Age of Mammals in the San Juan Basin, New Mexico: Biostratigraphy and Evolution of Paleocene Mammals of the Nacimiento Formation. New Mexico Museum of Natural History and Science, Bulletin 8.

Wilson, G.P., 2005. Mammalian Faunal Dynamics During the Last 1.8 Million Years of the Cretaceous in Garfield County, Montana. Journal of Mammalian Evolution, Vol. 12, Nos. ½, pp. 53-76.

Zijderveld, J.D.A., 1967. A.C. demagnetization of rocks: Analysis of results, in Collinson, D.W., et al., eds., Methods of palaeomagnetism, Amsterdam, Elsevier, pp. 254-286.

Appendix A - East Reid Coulee to Flag Butte Section

Bottom of Unit (m)	Top of Unit (m)	General Lithology	Description
0.000	15.354	mudstone	Unit 1: Middle Fox Hills mudstone
15.354	25.879	sandstone	Unit 2: Upper Fox Hills sandstone
25.879	26.879	redsandstone	Iron indurated layer between FH and HC
26.879	33.194	sandstone	Unit 3: Basal Hell Creek sandstone
33.194	54.306	paleosols	Unit 4: HC layered paleosols/siltstones
54.306	60.110	sandstone	HC sandstone 1
60.110	83.156	paleosols	Unit 4: HC layered paleosols/siltstones
83.156	99.872	sandstone	HC sandstone 2
99.872	103.641	siltstone	Grey siltstone
103.641	104.885	mudstone	Medium sand fining upward to mudstone
104.885	105.685	mudstone	Brown mudstone
105.685	107.133	siltstone	Carbonaceous siltstone
107.133	109.931	siltstone	Grey siltstone
109.931	114.067	sandstone	HC sandstone 3
114.067	115.667	mudstone	Grey mudstone
115.667	115.817	lignite	Small lignite
115.817	118.017	mudstone	Grey mudstone
118.017	119.039	lignite	K/Pg lignite

Appendix B - Pearl Lake Section

Bottom of Unit (m)	Top of Unit (m)	General Lithology	Description
5.343	5.793	lignite	Lower Z coal
5.793	6.908	siltstone	Grey laminated siltstone
6.908	7.208	sandstone	Unlaminated silty sandstone
7.208	8.108	sandstone	Channel sandstone
8.108	8.708	mudstone	Carbonaceous mudstone
8.708	8.824	mudstone	Grey mudstone
8.824	9.024	shale	Carbonaceous shale
9.024	9.824	siltstone	Grey/brown siltstone
9.824	10.924	lignite	Upper Z coal
10.924	17.406	sandstone	Massive cross-bedded sandstone
17.406	17.506	redsandstone	Carbonate sandstone-indurated
17.506	19.548	mudstone	Brownish-grey mudstone
19.548	20.197	shale	Carbonaceous shale
20.197	21.297	sandstone	Greyish sandstone
21.297	23.176	shale	Carbonaceous shale with mudstone
23.176	24.858	siltstone	Brownish-grey siltstone
24.858	25.658	siltstone	Grey siltstone
25.658	26.308	lignite	Y coal stringer
26.308	27.300	mudstone	Brownish-olive mudstone

Appendix C - Garbani Hill Section

Bottom of Unit (m)	Top of Unit (m)	General Lithology	Description
0.000	2.469	lignite	Y coal
2.469	7.821	sandstone	Tan/grey sandstone
7.821	10.421	sandstone	Grey, silty sandstone
10.421	10.821	lignite	X (?) coal
10.821	11.971	mudstone	Grey/brown mudstone
11.971	15.971	sandstone	Light grey silty sandstone
15.971	16.289	shale	Carbonaceous shale
16.289	21.115	mudstone	Grey to darker grey mudstone
21.115	22.265	siltstone	Brownish-grey siltstone
22.265	22.349	redsandstone	Red/tan sandstone

Appendix D - W-Coal Area to Biscuit Butte

Bottom of Unit (m)	Top of Unit (m)	General Lithology	Description
0.000	2.701	mudstone	Grey mudstone
2.701	2.901	sandstone	Red/orange capping sandstone
2.901	5.601	siltstone	greyish/tan siltstone
5.601	6.551	lignite	Lower W lignite
6.551	8.801	sandstone	Tan sandstone
8.801	10.239	lignite	Upper W lignite
10.239	14.091	siltstone	Grey carbonaceous siltstone
14.091	16.622	mudstone	Siltstone to mudstone
16.622	17.522	lignite	V (?) coal
17.522	20.007	siltstone	Olive/grey/orange siltstone
20.007	30.507	sandstone	Covered tan sandstone
30.507	32.177	lignite	U coal
32.177	36.851	mudstone	Brownish-grey mudstone